DOI: 10.1002/ejic.200500727

Molecular Structures and Magnetism of Mn_{12} Nanomagnets Containing the 3-Thiophenecarboxylate Ligand

Jin Mook Lim,[b] Youngkyu Do,[b] and Jinkwon Kim*[a]

Keywords: Single-molecule magnet / Mn_{12} complex / Molecular structure / Magnetic properties / Molecular films

The new Mn_{12} single-molecule magnets containing thiophenyl ligands, $[Mn_{12}O_{12}(O_2CC_4H_3S)_{16}(HO_2CC_4H_3S)(H_2O)_2]\cdot 5CH_2Cl_2$(**1**) and $[Mn_{12}O_{12}(O_2CC_4H_3S)_{16}(H_2O)_4]\cdot 6CH_2Cl_2\cdot 2H_2O$ (**2**), have been synthesized by ligand-substitution reactions of 3-thiophenecarboxylic acid and $[Mn_{12}O_{12}(O_2CCH_3)_{16}(H_2O)_4]$ and investigated by magnetic measurements with a SQUID magnetometer. The X-ray analysis of **1** shows five-coordination geometry around the Mn^{III} ion due to the unusual coordination of 3-thiophenecarboxylic acid to the Mn^{III} ion. Compound **1** displays two different rates of magnetization relaxation, which are faster than that of compound **2** because of structural distortion in the Mn_{12} complex of **1**. Magnetic susceptibility measurements on **1** and **2** give the following parameters: U_{eff} (the faster relaxation form of **1**) = 51.81 K, $1/\tau_0 = 1.90\cdot 10^8\ s^{-1}$; U_{eff} (the slower relaxation form of **1**) = 66.44 K, $1/\tau_0 = 1.50\cdot 10^8\ s^{-1}$; U_{eff}(**2**) = 67.09 K, $1/\tau_0 = 1.32\cdot 10^8\ s^{-1}$.

Introduction

Single-molecule magnets (SMMs) have been the subject of intensive investigation in the last years.[1] SMM behavior was first observed in $[Mn_{12}O_{12}(OAc)_{16}(H_2O)_4]$ ($Mn_{12}Ac$) in 1993.[2,3] SMMs display stepwise magnetization hysteresis loops below the blocking temperature due to a very slow magnetization relaxation rate as well as a resonant quantum tunneling of magnetization. SMMs also exhibit quantum phase interference. Therefore, SMMs are regarded as the elementary units in ultimate high-density magnetic storage[4] and in the design of quantum computers.[5,6] One the other hand, recent research reports showed that molecular clusters possessing quantized magnetic properties may provide powerful new systems for single-molecule transistors.[7,8]

Investigating individual molecules is essential for realizing the proposed application of SMMs. An approach to accomplishing this goal is to deposit SMMs on a suitable substrate and use scanning probe microscopy (SPM) to sense individual molecules. Various types of SPM techniques, such as scanning tunneling microscopy (STM), atomic force microscopy (AFM), and magnetic force microscopy (MFM) can be employed to verify the electronic, mechanical, and magnetic characterization of the molecules. Recently, various attempts have been made in preparation and SPM characterization: Langmuir–Blodgett (LB) films of Mn_{12} clusters,[9] MFM study on Mn_{12} complexes embedded in a polycarbonate matrix,[10] STM study of $[Mn_{12}O_{12}\{16\text{-(hydrothio)hexanecanoate}\}_{16}(H_2O)_4]$ organized on a gold surface,[11] stamp assisted deposition and patterning,[12] the preparation of monolayer and multilayer films on functionalized surfaces,[13] and study of molecular ordering and magnetism of $[Mn_{12}O_{12}(t\text{BuCO}_2)_{16}(H_2O)_4]$ on a gold surface.[14] Very recently, grafting of Mn_{12} complexes on a Si surface have been reported.[15,16] However, the methodology for depositing SMMs with monolayer or submonolayer coverage on a useful substrate such as silicon or gold is not yet well established, and the direct measurement of the characteristics of individual molecules of SMMs is still in the beginning stage. Therefore, we designed a new Mn_{12} complex with surface-adhesive functional groups in peripheral ligands to give molecular monolayers on a gold surface. Here we report the synthesis, structure, and magnetic properties of Mn_{12} complexes containing the thiophenyl group, $[Mn_{12}O_{12}(O_2CC_4H_3S)_{16}(HO_2CC_4H_3S)(H_2O)_2]\cdot 5CH_2Cl_2$ (**1**) and $[Mn_{12}O_{12}(O_2CC_4H_3S)_{16}(H_2O)_4]\cdot 6CH_2Cl_2\cdot 2H_2O$ (**2**).

Results and Discussion

Synthesis

The ligand-substitution reaction of $Mn_{12}Ac$ with 3-thiophenecarboxylic acid has been carried out by a modified azeotropic distillation method.[17] Most ligand-substitution reactions have been performed with a large excess of RCOOH. However, in our modified method, only a stoichiometric amount of 3-thiophenecarboxylic acid was al-

[a] Department of Chemistry, Kongju National University, 182 Shinkwan, Kongju, Chungnam 314-701, Korea
Fax: + 82-41-850-8479
E-mail: jkim@kongju.ac.kr
[b] Department of Chemistry, School of Molecular Science BK21 and Center for Molecular Design and Synthesis, KAIST, 373-1 Guseong-dong, Yuseong-gu, Daejeon 305-701, Korea

lowed to react with $Mn_{12}Ac$. The solubility of $Mn_{12}Ac$ is very poor in dichloromethane. Nevertheless, as $Mn_{12}Ac$ reacts with 3-thiophenecarboxylic acid, the color of the solution darkens, indicating that the ligand-substitution reaction proceeds. To complete the substitution reaction, toluene was added to the reaction mixture and evaporated to remove acetic acid as the toluene azeotrope. The reaction of $Mn_{12}Ac$ with 17 equiv. of 3-thiophenecarboxylic acid gives complex **1**, whereas complex **2** is obtained by a reaction with 16 equiv. 3-thiophenecarboxylic acid. Complex **1** has a 3-thiophenecarboxylic acid as terminal coordination ligand which can be substituted by a water molecule. Complex **1** is converted to complex **2** by recrystallization in wet CH_2Cl_2/hexane mixed solvent.

Molecular Structures

An ORTEP diagram of $[Mn_{12}O_{12}(O_2CC_4H_3S)_{16}(HO_2CC_4H_3S)(H_2O)_2]$ is shown in Figure 1. Selected bond parameters are listed in Table 1 and Table 2. Complex **1** has unusual molecular structure compared with other normal Mn_{12}–carboxylate species. Mn_{12}–carboxylate complexes usually have sixteen carboxylates as peripheral bridging ligands which bridge the outer-ring Mn^{III} atoms to both the inner Mn^{IV} and the other outer-ring Mn^{III} atoms. Four water molecules are coordinated to the outer-ring Mn^{III} atoms. Complex **1** has sixteen 3-thiophenecarboxylates as peripheral bridging ligands, but it abnormally has one 3-thiophenecarboxylic acid and only two water molecules as terminal coordination ligands to Mn^{III} ions. As a result of the coordination of 3-thiophenecarboxylic acid, the Mn^{III} ion (Mn6) has highly distorted five-coordination geometry. The octahedral Mn^{III}–O bonds of $[Mn_{12}O_{12}]$ complexes are tetragonally elongated because of a Jahn–Teller distortion. An elongation axis is usually parallel to the molecular C_2 axis. However, there is no such elongation at Mn6 because of its five-coordination geometry. The longest Mn^{III}–O bond length around Mn6 is 2.067(7) Å, which is significantly shorter than the axially elongated Mn^{III}–O bond lengths (2.096–2.218 Å) of the six-coordinate Mn^{III} atoms. Bond angles of O7–Mn6–O38 and O14–Mn6–O38 are 101.4(3)° and 92.8(3)°, respectively. Examples of five-coordinate Mn^{III} atoms in Mn_{12} complexes are quite rare and only observed previously in $[Mn_{12}O_{12}(O_2CEt)_{16}(H_2O)_3]$.[18] The two water molecules are located on the two Mn atoms (Mn8 and Mn12) to complete octahedral coordination.

The structure of complex **2** is quite similar in many respects to the previously characterized Mn_{12} complexes. Complex **2** has normal $[Mn_{12}O_{12}]^{16+}$ core structure, as shown in Figure 2 and Figure 3, possessing four water ligands bound to three Mn centers (Mn8, Mn10, Mn12) with a 1:1:2 arrangement. All Jahn–Teller elongation axes of eight Mn^{III} centers of both complexes are oriented approximately in the axial direction.

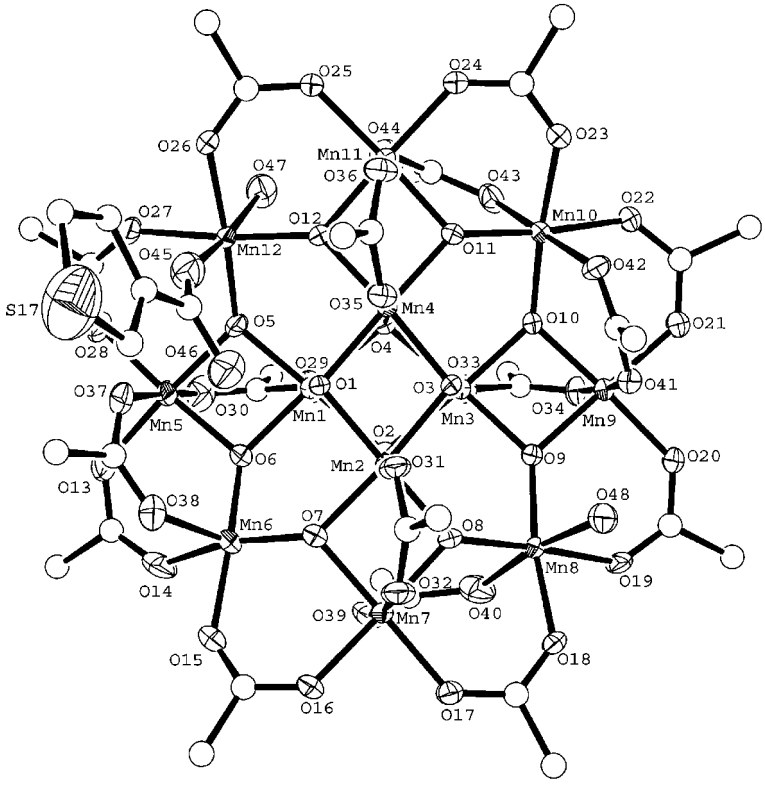

Figure 1. ORTEP representation of the Mn_{12} complex of **1** showing 50% probability ellipsoids. For clarity, thiophenyl groups of the 3-thiophenecarboxylate bridging ligands are omitted.

Table 1. Selected bond lengths [Å] in **1**.

A	B	Bond length	A	B	Bond length
Mn(1)	O(1)	1.919(6)	Mn(1)	O(2)	1.898(5)
Mn(1)	O(4)	1.903(5)	Mn(1)	O(5)	1.877(5)
Mn(1)	O(6)	1.870(6)	Mn(1)	O(29)	1.908(7)
Mn(2)	O(1)	1.924(5)	Mn(2)	O(2)	1.906(6)
Mn(2)	O(3)	1.931(5)	Mn(2)	O(7)	1.889(6)
Mn(2)	O(8)	1.853(5)	Mn(2)	O(31)	1.900(6)
Mn(3)	O(2)	1.912(5)	Mn(3)	O(3)	1.897(6)
Mn(3)	O(4)	1.921(5)	Mn(3)	O(9)	1.867(5)
Mn(3)	O(10)	1.864(5)	Mn(3)	O(33)	1.920(6)
Mn(4)	O(1)	1.938(5)	Mn(4)	O(3)	1.903(5)
Mn(4)	O(4)	1.908(6)	Mn(4)	O(11)	1.850(5)
Mn(4)	O(12)	1.860(5)	Mn(4)	O(35)	1.903(6)
Mn(5)	O(5)	1.905(6)	Mn(5)	O(6)	1.899(6)
Mn(5)	O(13)	1.957(7)	Mn(5)	O(28)	1.927(6)
Mn(5)	O(30)	2.181(8)	Mn(5)	O(37)	2.096(8)
Mn(6)	O(6)	1.859(6)	Mn(6)	O(7)	1.893(6)
Mn(6)	O(14)	1.943(8)	Mn(6)	O(15)	1.926(7)
Mn(6)	O(38)	2.067(7)	Mn(7)	O(7)	1.915(6)
Mn(7)	O(8)	1.895(6)	Mn(7)	O(16)	1.951(6)
Mn(7)	O(17)	1.951(6)	Mn(7)	O(32)	2.196(7)
Mn(7)	O(39)	2.135(7)	Mn(8)	O(8)	1.898(6)
Mn(8)	O(9)	1.873(5)	Mn(8)	O(18)	1.944(6)
Mn(8)	O(19)	1.963(6)	Mn(8)	O(40)	2.111(7)
Mn(8)	O(48)	2.218(7)	Mn(9)	O(9)	1.898(5)
Mn(9)	O(10)	1.887(5)	Mn(9)	O(20)	1.932(6)
Mn(9)	O(21)	1.945(6)	Mn(9)	O(34)	2.174(7)
Mn(9)	O(41)	2.168(7)	Mn(10)	O(10)	1.877(6)
Mn(10)	O(11)	1.911(5)	Mn(10)	O(22)	1.980(6)
Mn(10)	O(23)	1.936(6)	Mn(10)	O(42)	2.135(7)
Mn(10)	O(43)	2.189(6)	Mn(11)	O(11)	1.892(5)
Mn(11)	O(12)	1.890(5)	Mn(11)	O(24)	1.945(6)
Mn(11)	O(25)	1.945(6)	Mn(11)	O(36)	2.208(6)
Mn(11)	O(44)	2.178(7)	Mn(12)	O(5)	1.887(6)
Mn(12)	O(12)	1.880(6)	Mn(12)	O(27)	1.938(6)
Mn(12)	O(26)	1.941(6)	Mn(12)	O(45)	2.198(8)
Mn(12)	O(47)	2.216(7)			

Table 2. Selected bond lengths [Å] in **2**.

A	B	Bond length	A	B	Bond length
Mn(1)	O(1)	1.904(5)	Mn(1)	O(2)	1.932(5)
Mn(1)	O(4)	1.925(5)	Mn(1)	O(5)	1.892(5)
Mn(1)	O(6)	1.852(5)	Mn(1)	O(29)	1.911(5)
Mn(2)	O(1)	1.920(5)	Mn(2)	O(2)	1.901(5)
Mn(2)	O(3)	1.926(5)	Mn(2)	O(7)	1.873(5)
Mn(2)	O(8)	1.864(5)	Mn(2)	O(31)	1.912(5)
Mn(3)	O(2)	1.925(5)	Mn(3)	O(3)	1.911(5)
Mn(3)	O(4)	1.929(5)	Mn(3)	O(9)	1.886(5)
Mn(3)	O(10)	1.868(5)	Mn(3)	O(33)	1.932(5)
Mn(4)	O(1)	1.926(5)	Mn(4)	O(3)	1.904(5)
Mn(4)	O(4)	1.899(5)	Mn(4)	O(11)	1.887(5)
Mn(4)	O(12)	1.870(5)	Mn(4)	O(35)	1.936(5)
Mn(5)	O(5)	1.920(5)	Mn(5)	O(6)	1.878(5)
Mn(5)	O(13)	1.932(5)	Mn(5)	O(28)	1.945(6)
Mn(5)	O(30)	2.216(6)	Mn(5)	O(37)	2.204(6)
Mn(6)	O(6)	1.890(5)	Mn(6)	O(7)	1.929(5)
Mn(6)	O(14)	1.983(6)	Mn(6)	O(15)	1.976(5)
Mn(6)	O(38)	2.117(6)	Mn(6)	O(40)	2.104(6)
Mn(7)	O(7)	1.895(5)	Mn(7)	O(8)	1.888(5)
Mn(7)	O(16)	1.944(5)	Mn(7)	O(17)	1.941(5)
Mn(7)	O(32)	2.226(6)	Mn(7)	O(39)	2.198(6)
Mn(8)	O(8)	1.890(5)	Mn(8)	O(9)	1.899(5)
Mn(8)	O(18)	1.972(5)	Mn(8)	O(19)	1.966(5)
Mn(8)	O(42)	2.101(6)	Mn(8)	O(47)	2.227(6)
Mn(9)	O(9)	1.902(5)	Mn(9)	O(10)	1.880(5)
Mn(9)	O(20)	1.926(5)	Mn(9)	O(21)	1.938(5)
Mn(9)	O(34)	2.237(6)	Mn(9)	O(41)	2.199(5)
Mn(10)	O(10)	1.889(5)	Mn(10)	O(11)	1.902(5)
Mn(10)	O(22)	1.944(5)	Mn(10)	O(23)	1.977(5)
Mn(10)	O(43)	2.119(6)	Mn(10)	O(48)	2.216(6)
Mn(11)	O(11)	1.905(5)	Mn(11)	O(12)	1.879(5)
Mn(11)	O(24)	1.919(5)	Mn(11)	O(25)	1.941(5)
Mn(11)	O(36)	2.222(6)	Mn(11)	O(44)	2.219(5)
Mn(12)	O(5)	1.888(5)	Mn(12)	O(12)	1.873(5)
Mn(12)	O(26)	1.978(6)	Mn(12)	O(27)	1.941(6)
Mn(12)	O(45)	2.204(6)	Mn(12)	O(46)	2.192(6)

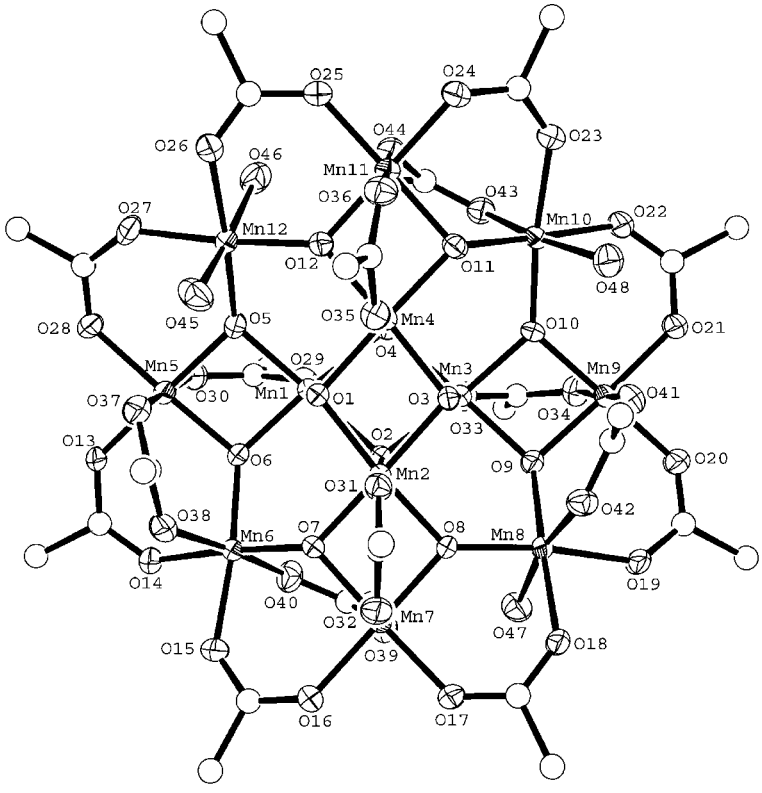

Figure 2. ORTEP representation of the Mn_{12} complex of **2** showing 50% probability ellipsoids. For clarity, thiophenyl groups of the 3-thiophenecarboxylate bridging ligands are omitted.

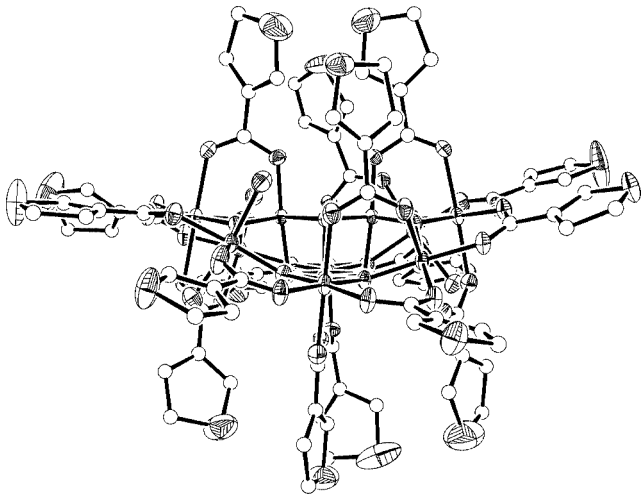

Figure 3. Side view of complex **2**.

Magnetic Properties

Out-of-phase ac magnetic susceptibility (χ_M'') measurements were carried out in the region of 2 to 10 K at zero dc field. As shown in Figure 4, frequency-dependent χ_M'' peaks in the 4–7 K region of **1** are less symmetric compared with those of **2**, and the shoulders in the 3–6 K region indicate a chemical species having a faster relaxation rate of quantum tunneling of magnetization.

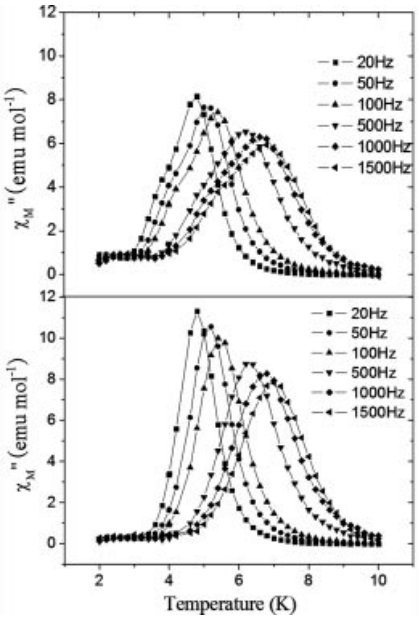

Figure 4. Comparison of out-of phase ac susceptibility signals of **1** (top) and **2** (bottom).

Magnetization relaxation rates ($1/\tau$) and effective anisotropy energy barriers were calculated from the theoretical Equation (1) given by

$$\ln(1/\tau) = -U_{eff}/kT + \ln(1/\tau_0) \quad (1)$$

where U_{eff} is the effective anisotropy energy barrier, k is the Boltzmann constant, and T is the temperature. Magnetic relaxation times (τ) are obtained from the relationship $\omega\tau = 1$ at the maxima of the χ_M'' vs. T plots. Peak maxima are accurately determined by fitting the peaks to a Lorentzian function. Figure 5 displays deconvolution of out-of-phase ac susceptibilities of **1** at 20 Hz. A least-squares fit (Figure 6) of ac susceptibility relaxation data to Equation (1) for faster-relaxation and slower-relaxation forms of **1** as well as **2** gives the following parameters: U_{eff} (the faster-relaxation form of **1**) = 51.81 K; $1/\tau_0 = 1.90 \cdot 10^8$ s^{-1}, U_{eff} (the slower-relaxation form of **1**) = 66.44 K; $1/\tau_0 = 1.50 \cdot 10^8$ s^{-1}, U_{eff}(**2**) = 67.09 K, $1/\tau_0 = 1.32 \cdot 10^8$ s^{-1}.

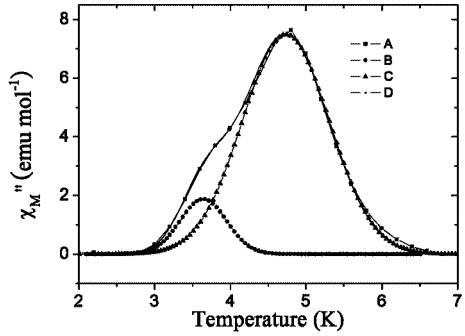

Figure 5. Deconvolution of ac susceptibilities of **1** at 20 Hz. A: original plot, B: deconvoluted low-temperature form, C: deconvoluted high-temperature form, D: sum of B and C.

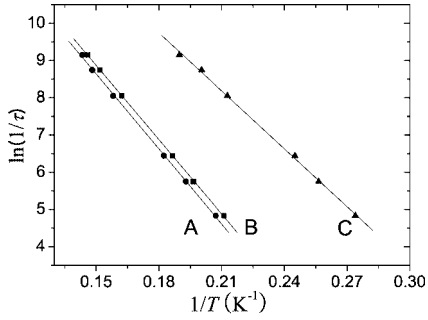

Figure 6. Arrhenius Plots of the natural logarithm of relaxation rate, $\ln(1/\tau)$ vs. inverse temperature for **1** and **2**. A: **2**, B: high temperature form of **1**, C: low temperature form of **1**.

The relaxation rate of the Mn_{12} SMM is dependent on the structural distortion of the Mn_{12} species because the rate of tunneling is determined by transverse magnetic fields (either outside or inside the molecule) or by transverse higher-order zero-field interaction terms.[19] Dislocations should be an external source of spin tunneling in Mn_{12} crystals.[20] Jahn–Teller isomerism[21] is proposed as an internal source causing the tunneling rate of the Mn_{12} species to increase. An example of Jahn–Teller isomerism can be given by mentioning the compounds $[Mn_{12}O_{12}(O_2CC_6H_4Me\text{-}4)_{16}(H_2O)_4]\cdot HO_2CC_6H_4Me\text{-}4$[19] and $[Mn_{12}O_{12}(O_2CPh\text{-}4\text{-}SMe)_{16}(H_2O)_4]\cdot 7CH_2Cl_2$,[17c] which have an equatorially elongated axis and predominantly a χ_M'' peak in the region 2–4 K. Solvent molecules in the crystal lattice, which might be an external factor influencing the rate of tunneling, also affect the tunneling rate. For example, different tunneling rates were observed in the Mn_{12}–propionate complexes $[Mn_{12}O_{12}(O_2CCH_2CH_2Cl)_{16}(H_2O)_4]\cdot 0.5CH_2Cl_2\cdot 2H_2O$ and

$[Mn_{12}O_{12}(O_2CCH_2CH_2Cl)_{16}(H_2O)_4]\cdot CH_2ClCH_2CO_2H$.[22] As shown in Figure 6, the rate of quantum tunneling in the magnetization of **1** is a little bit faster than that of **2** because of the unusual five-coordination around the Mn6 ion as well as the ligation of 3-thiophenecarboxylates in complex **1**. Such structural distortions can be regarded as an internal source that increases the rate of quantum tunneling.

Hysteresis loops for **1** (filled squares) and **2** (open circles) at 2 K are shown in Figure 7 (left). Small plateaus for both complexes are observed in the hysteresis loops because of quantum tunneling of magnetization (QTM). To clarify the positions of QTM, plots of dM/dH vs. H are drawn in Figure 7 (right). QTM occurs at the field of each peak. Plots of reduced magnetization ($M/N\mu_B$) as a function of H/T, where N is Avogadro's number and μ_B is the Bohr magneton, were also obtained for compounds **1** and **2**. The data were fitted to the basic thermodynamic expression given in Equation (2), which takes the full power of the average of the magnetization into account:[23]

$$M = -\frac{N}{4\pi}\int_0^{2\pi}\int_0^{\pi}\frac{\sum_p (dE_p/dH)\exp(-E_p/k_BT)}{\sum_p \exp(-E_p/k_BT)} \times \sin\theta d\theta d\phi \quad (2)$$

In Equation (2), k_B is the Boltzmann constant and E_p is the eigenenergy obtained by diagonalization of the spin Hamiltonian matrix, including axial zero-field splitting and Zeeman interactions. The plots of reduced magnetization ($M/N\mu_B$) vs. H/T fitted well with $S = 10$, $g = 1.84$, and $D = 0.61$ K for **1** and $S = 10$, $g = 1.86$, and $D = 0.65$ K for **2**.

The sulfur atoms of **2** are directed toward the outside and are able to form strong bonds to the gold surface. A molecular thin film of **2** was prepared by immersing atomically flat gold substrates in a 0.1 mM solution of **2** in toluene for more than 5 minutes. The atomically flat gold substrates were prepared by electron-beam evaporation of gold on mica at 300 °C and subsequent annealing at 500 °C for 30 minutes. XPS analysis was performed to determine the composition and the chemical state of the film of compound **2** on Au(111). A survey spectrum clearly displays the photoelectron peaks for manganese, sulfur, oxygen, carbon, and gold. Figure 8 shows the high-resolution spectrum of the Mn 2p region for the Mn12 film. The Mn $2p_{1/2}$ and $2p_{3/2}$ and peaks are observed at 654 eV and 642 eV, respectively, and are consistent with the values observed with the Mn12–ac crystal.[24] The surface morphology of the film has been investigated by STM and AFM.[25,26] These studies indicate that the thiophenyl group can be used to anchor the Mn_{12} complex to the Au surface and demonstrate that individual molecules can be addressed and their physical properties can be investigated by using the SPM techniques. We plan to conduct an STM experiment at low temperatures of the SMM at the molecular level and eventually devise a strategy for the application of the SMM to quantum devices.

Conclusions

The syntheses and X-ray structures of $[Mn_{12}O_{12}(O_2CC_4H_3S)_{16}(HO_2CC_4H_3S)(H_2O)_2]\cdot 5CH_2Cl_2$ (**1**) and $[Mn_{12}O_{12}(O_2CC_4H_3S)_{16}(H_2O)_4]\cdot 6CH_2Cl_2\cdot 2H_2O$ (**2**) are reported. There is a distorted five-coordination site due to the very unusual coordination of 3-thiophenecarboxylic acid as a terminal ligand in complex **1**. Complex **2** has normal coordination geometry. Such an internal structure distortion of **1** causes faster relaxation of magnetization in **1** relative to **2**. A molecular thin film of the Mn12 SMM has been successfully fabricated by using complex **2**. The molecules

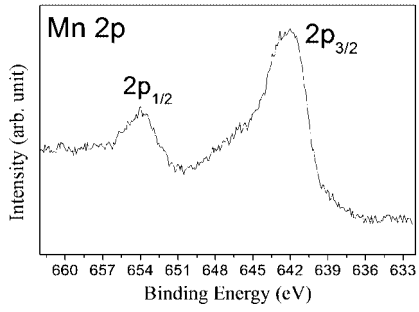

Figure 8. Photoelectron spectrum of Mn 2p core-level obtained from the film of compound **2** on Au(111) surface.

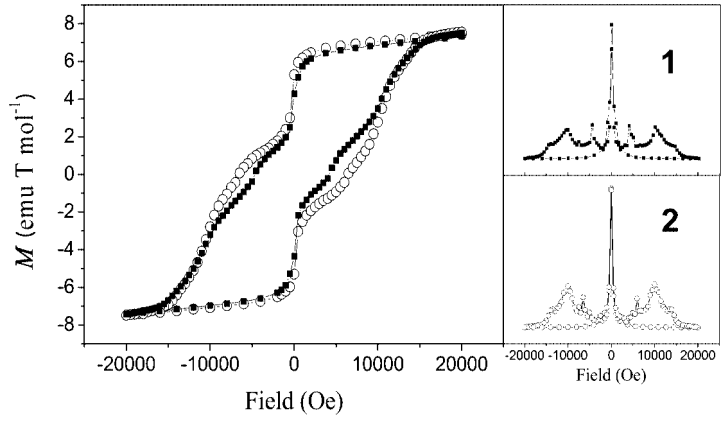

Figure 7. Hysteresis loops (left) and dM/dH plots (right) of **1** (■) and **2** (○) at 2 K.

of **2** are anchored on a gold surface strongly through sulfur atoms of 3-thiophenecarboxylate ligands.

Experimental Section

General Remarks: $Mn_{12}Ac$ was prepared according to a published procedure.[27] All reagents and solvents were purchased from commercial sources and used as received.

Physical Measurements: Elemental analyses were carried out by the Analytical Laboratory of the Korea Basic Science Institute, Seoul. Infrared spectra were recorded with a Perkin–Elmer 16 PC spectrophotometer. Variable-temperature magnetic susceptibility measurements were carried out on powder samples of complex **1** and complex **2** using a Quantum Design MPMS*XL* susceptometer well equipped with a 50-kG magnet. The samples were introduced into the XPS chamber by means of a load lock system. The base pressure was $1 \cdot 10^{-10}$ Torr. All XPS spectra were recorded with a VG Scientific ESCALAB MK II spectrometer using an Al-K_α source run at 15 kV and 10 mA. The binding energy scale was calibrated to 284.6 eV for the main C 1s peak. Each sample was analyzed at a 90° angle relative to the electron analyzer. The ac field range was $1 \cdot 10^{-4}$ to 5 Oe, oscillating at a frequency in the range $5 \cdot 10^{-4}$ to 1512 Hz. The sets of ac susceptibility data were collected for the powdered, microcrystalline sample in an ac field of 3.0 Oe, oscillating in the 20–1500 Hz range. The samples were aligned in eicosane with an applied dc field of 5 T at a temperature above the melting point of eicosane for 15 min. Corrections for the diamagnetism of the complexes were estimated using Pascal's constants, and magnetic data were corrected for diamagnetic contributions of the sample holder.

Synthesis of Complex 1: A slurry of $Mn_{12}Ac$ (206 mg, 0.1 mmol) in dichloromethane (30 ml) was stirred with 3-thiophenecarboxylic acid (230 mg, 1.8 mmol) for 4 h at room temperature to give a dark blown solution. Azeotropic distillation with toluene (20 ml) was performed six times to completely remove the released acetic acid, and the resultant dark brown solid was dissolved in dichloromethane and filtered. The filtrate was allowed to diffuse with pentane vapor. After a week, black crystals of **1** were collected by filtration and washed with hexane. FTIR data: 1561(s), 1522(s), 1439(s), 1358(s), 1319(s), 1208(w), 1120(w), 1073(w), 940(w), 873(w), 833(W), 754(s), 702(m), 658(m), 628(m), 517(m) cm^{-1}. $C_{90}H_{66}Cl_{10}Mn_{12}O_{48}S_{17}$ (3474.23): calcd. C 33.48, H 1.85, S 17.87; found C 33.41, H 1.95, S 18.21.

Synthesis of Complex 2: Complex **2** was synthesized in the same manner as complex **1** except that 16 equiv. 3-thiophenecarboxylic acid (215 mg, 1.8 mmol) was treated with $Mn_{12}Ac$ (205 mg, 0.1 mmol) in dichloromethane (30 mL). After several azeotropic distillations, the dark brown product was recrystalized from dichloromethane/hexane to give complex **2**. $C_{86}H_{72}Cl_{12}Mn_{12}O_{50}S_{16}$ (3503.08): calcd. C 32.10, H 2.02, S 17.14; found C 31.78, H 2.11, S 17.26.

Crystal Structure Determination: Reflection data were collected with a Bruker SMART CCD diffractometer using monochromated Mo-K_α (λ = 0.71073 Å) radiation. The data were integrated and scaled using the SAINT software package.[28] Collected data were corrected for absorbance by using SADABS[28] based upon the Laue symmetry using equivalent reflections. Structures ware solved by the direct method and refined by least-squares calculations with the SHELXL-PLUS 5.05 software package.[29] The non-hydrogen atoms were refined anisotropically, and the geometrically restrained hydrogen atoms were treated using an appropriate riding model. A summary of the crystallographic parameters and data is given in Table 3. The proposed models include disorders of the thiophene rings and solvent molecules.

CCDC-280093 and CCDC-280094 contain the supplementary crystallographic data for this paper. These data can be obtained free of charge from The Cambridge Crystallographic Data Centre via www.ccdc.cam.ac.uk/data_request/cif.

Acknowledgments

This work was supported by the NRL program of the Ministry of Science and Technology, Korea.

[1] D. Gatteschi, R. Sessoli, *Angew. Chem. Int. Ed.* **2003**, *42*, 268.
[2] R. Sessoli, D. Gatteschi, A. Caneschi, M. A. Novak, *Nature* **1993**, *365*, 141.
[3] R. Sessoli, H.-L. Tsai, A. R. Schake, S. Wang, J. B. Vincent, K. Folting, D. Gatteschi, G. Christou, D. N. Hendrickson, *J. Am. Chem. Soc.* **1993**, *115*, 1804.

Table 3. Details of crystallographic data collection for **1** and **2**.

	1	**2**
Chemical formula	$C_{90}H_{66}Cl_{10}Mn_{12}O_{48}S_{17}$	$C_{86}H_{72}Cl_{12}Mn_{12}O_{50}S_{16}$
Chemical formula weight	3474.23	3503.08
Space group	$P\bar{1}$	$P\bar{1}$
a [Å]	17.552(1)	15.993(1)
b [Å]	17.936(1)	16.396(1)
c [Å]	23.957(2)	25.628(2)
α [°]	78.790(2)	79.748(1)
β [°]	76.300(2)	85.147(1)
γ [°]	64.885(2)	80.856(1)
V [Å^3]	6596.9(9)	6517.9(7)
Z	2	2
$\rho_{calcd.}$ [g cm^{-3}]	1.749	1.785
μ [mm^{-1}]	1.658	1.704
No. of unique reflections	28359	28387
No. of observed reflections	13369 [$I_o > 2\sigma(I_o)$]	18224 [$I_o > 2\sigma(I_o)$]
$2\theta_{max}$ [°]	56	56
No. of parameters refined	1696	1603
$R(F)$, $wR(F_2)$	0.0861, 0.2503	0.0883, 0.2645
GOF	0.968	1.023

[4] L. Krusin-Elbaum, T. Shibauchi, B. Argyle, L. Gignac, D. Weller, *Nature* **2001**, *410*, 444.
[5] J. Tejada, E. M. Chudnovsky, E. del Barco, J. M. Hernandez, T. P. Spiller, *Nanotechnology* **2001**, *12*, 181.
[6] B. Zhou, R. Tao, S.-Q. Shen, J.-Q. Liang, *Phys. Rev. A* **2002**, *66*, 010301(R).
[7] G.-H. Kim, T.-S. Kim, *Phys. Rev. Lett.* **2004**, *92*, 137203.
[8] W. Liang, M. P. Shores, M. Bockrath, J. R. Long, H. Park, *Nature* **2002**, *417*, 725.
[9] M. Clemente-León, H. Soyer, E. Coronado, C. Mingotaud, C. J. Gómez-García, P. Delhaès, *Angew. Chem. Int. Ed.* **1998**, *37*, 2841.
[10] D. Ruiz-Molina, M. Mas-Torrent, J. Gomez, A. I. Balana, N. Domingo, J. Tejada, M. T. Martinez, C. Rovira, J. Veciana, *Adv. Mater.* **2003**, *15*, 42.
[11] A. Cornia, A. C. Fabretti, M. Pacchioni, L. Zobbi, D. Bonacchi, A. Caneschi, D. Gatteschi, R. Biagi, U. Del Pennino, V. De Renzi, L. Gurevich, H. S. J. Van der Zant, *Angew. Chem. Int. Ed.* **2003**, *42*, 1645.
[12] M. Cavallini, F. Biscarini, J. Gomez-Segura, D. Ruiz, J. Veciana, *Nano Lett.* **2003**, *3*, 1527.
[13] J. S. Steckel, N. S. Persky, C. R. Martinez, C. L. Barnes, E. A. Fry, J. Kulkarni, J. D. Burgess, R. B. Pacheco, S. L. Stoll, *Nano Lett.* **2004**, *4*, 399.
[14] A. Naitabdi, J.-P. Bucher, P. Gerbier, P. Rabu, M. Drillon, *Adv. Mater.* **2005**, *17*, 1612.
[15] G. G. Condorelli, A. Motta, I. L. Fragalà, F. Giannazzo, V. Raineri, A. Caneschi, D. Gatteschi, *Angew. Chem. Int. Ed.* **2004**, *43*, 4081.
[16] B. Fleury, L. Catala, V. Huc, C. David, W. Z. Zhong, P. Jegou, L. Baraton, S. Palacin, P.-A. Albouy, T. Mallah, *Chem. Commun.* **2005**, 2002.
[17] a) H. J. Eppley, H.-L. Tsai, N. de Vries, K. Folting, G. Christou, D. N. Hendrickson, *J. Am. Chem. Soc.* **1995**, *117*, 301; b) W. Jeon, M. K. Jin, Y. Kim, D.-Y. Jung, B. J. Suh, S. Yoon, *Bull. Korean Chem. Soc.* **2004**, *25*, 1036; c) J. M. Lim, Y. Do, J. Kim, *Bull. Korean Chem. Soc.* **2005**, *26*, in press.
[18] H. J. Eppley, H.-L. Tsai, N. de Vries, K. Folting, G. Christou, D. N. Hendrickson, *J. Am. Chem. Soc.* **1995**, *117*, 301.
[19] Z. Sun, D. Ruiz, E. Rumberger, C. D. Incarvito, K. Folting, A. L. Rheingold, G. Christou, D. N. Hendrickson, *Inorg. Chem.* **1998**, *37*, 4758.
[20] D. A. Garanin, E. M. Chudnovsky, *Phys. Rev. B* **2002**, *65*, 94423.
[21] S. M. J. Aubin, Z. Sun, H. J. Eppley, E. M. Rumberger, I. A. Guzei, K. Folting, P. K. Gantzel, A. L. Rheingold, G. Christou, D. N. Hendrickson, *Inorg. Chem.* **2001**, *40*, 2127.
[22] C.-D. Park, S. W. Rhee, Y. Kim, W. Jeon, D.-Y. Jung, D. Kim, Y. Do, H.-C. Ri, *Bull. Korean Chem. Soc.* **2001**, *22*, 453.
[23] V. Vermaas, W. L. Groeneveld, *Chem. Phys. Lett.* **1974**, *27*, 583.
[24] J.-S. Kang, J. H. Kim, Y. J. Km, W. S. Jeon, D.-Y. Jung, S. W. Han, K. H. Kim, K. J. Kim, B. S. Kim, *J. Korean Phys. Soc.* **2002**, *40*, L402.
[25] B. J. Kim, B. J. Suh, S. Yoon, S. H. Phark, Z. G. Khim, J. Kim, J. M. Lim, Y. Do, *J. Korean Phys. Soc.* **2004**, *45*, 1593.
[26] S. Phark, Z. G. Khim, B. J. Kim, B. J. Suh, S. Yoon, J. Kim, J. M. Lim, Y. Do, *Jpn. J. Appl. Phys., Part 1* **2004**, *43*, 8273.
[27] T. Lis, *Acta Crystallogr. Sect. B: Struct. Sci.* **1980**, *36*, 2042.
[28] Bruker AXS: Madison, WI, **1997**.
[29] R. H. Blessing, *Acta Crystallogr., Sect. A: Found. Crystallogr.* **1995**, *51*, 33.

Received: August 16, 2005
Published Online: January 3, 2006

